

Observational Constraints on the ICM Temperature Enhancement by Cluster Mergers

N. Okabe¹ and K. Umetsu²

¹ Astronomical Institute, Tohoku University, Aramaki, Aoba-ku, Sendai, 980-8578, Japan okabe@astr.tohoku.ac.jp

² Academia Sinica Institute of Astronomy and Astrophysics (ASIAA) P.O. Box 23-141, Taipei 106, Taiwan, R.O.C. keiichi@asiaa.sinica.edu.tw

Abstract

We present results from a combined weak lensing and X-ray analysis of the merging cluster A1914 at a redshift of $z = 0.1712$ based on R -band imaging data with Subaru/Suprime-Cam and archival Chandra X-ray data. Based on the weak-lensing and X-ray data we explore the relationships between cluster global properties, namely the gravitational mass, the bolometric X-ray luminosity and temperature, the gas mass and the gas mass fraction, as a function of radius. We found that the gas mass fractions within r_{2500} and r_{vir} are consistent with the results of earlier X-ray cluster studies and of cosmic microwave background studies based on the WMAP observations, respectively. However, the observed temperature, $k_B T_{\text{ave}} = 9.6 \pm 0.3 \text{keV}$, is significantly higher than the virial temperature, $k_B T_{\text{vir}} = 4.7 \pm 0.3 \text{keV}$ derived from the weak lensing distortion measurement. The X-ray bolometric luminosity and temperature ($L_X - T$) relation is consistent with the $L_X - T$ relation derived by previous statistical X-ray studies of galaxy clusters. Such correlations among the global cluster properties are invaluable observational tools for studying the cluster merger physics. Our results demonstrate that the combination of X-ray and weak-lensing observations is a promising, powerful probe of the physical processes associated with cluster mergers as well as of their mass properties.

1 Weak Lensing and X-ray Analyses

Weak Lensing Analysis

Weak lensing provides a direct measure of the projected mass distribution in the universe regardless of the physical/dynamical state of matter in the system. Therefore weak lensing enables the direct study of mass in clusters even when the clusters are in the process of (pre/mid/post) merging, where the assumptions of hydrostatic equilibrium or isothermality are no longer valid. We carried out a weak lensing analysis on the merging cluster A1914 with deep R_c -band data taken with Suprime-Cam on the Subaru telescope, covering the entire cluster region out to the cluster virial ra-

dius thanks to the wide field-of-view of $34' \times 27'$. The details of the analysis will be presented in Okabe & Umetsu [4] and Umetsu & Okabe[6]. We define a sample of background galaxies with magnitudes $21 \lesssim R_c \lesssim 26$ and r_h and half-light radii $r_h^* \lesssim r_h \lesssim 15$ pixels, yielding a mean galaxy number density of $n_g \simeq 48 \text{arcmin}^{-2}$. We derived a radial profile of the tangential component of reduced gravitational shear, $g_+ = \gamma_+ / (1 - \kappa)$, over the radial range of $3'$ to $17'$, where the irregularity in the mass distribution is less significant than that in the central region. The best-fitting NFW (Navarro, Frenk, & White[3]) profile to the Subaru distortion data is obtained as follows: virial mass $M_{\text{vir}} = (7.66 \pm 0.73) \times 10^{14} M_{\odot} h_{70}^{-1}$ (or virial radius $r_{\text{vir}} = 12'.26 = 2.144 h_{70}^{-1} \text{Mpc}$); concentration parameter $c = 5.07 \pm 1.75$. The best-fitting mass profile from weak lensing distortion measurements is in good agreement with the luminosity profile of cluster member galaxies, which will be presented in Umetsu & Okabe [6].

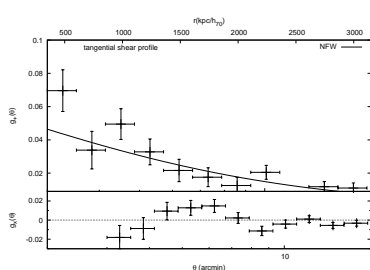


Fig. 1. Radial profiles of the reduced tangential shear (upper panel) and the 45° rotated (\times) component (lower panel). The solid curve represents the best-fitting NFW shear profile.

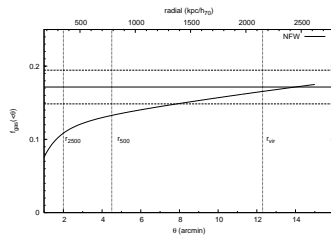


Fig. 2. Radial profile of the cluster gas mass fraction, f_{gas} , obtained by combining best fit results of weak lensing and X-ray analyses. Dashed vertical lines indicate the 1σ confidence range of the cosmic baryon fraction.

X-ray Analysis

We used archival *Chandra* data to measure physical properties of the ICM in A1914. We performed a spectral fit with a single temperature model within a radius of $5'$. The average temperature and abundance were obtained as $k_B T_{\text{ave}}(\theta < 5') = 9.6 \pm 0.3 \text{keV}$ $A = 0.19 \pm 0.08$ at a 90% confidence level, respectively. The radial profile fit was performed on the observed X-ray surface brightness distribution ($\theta < 6'$) using a single β model, where we adopted the same center as for the weak lensing tangential shear measurement. The best fitting parameters were obtained as follows: cluster core radius, $r_c = 1'.03 \pm 0'.06$; slope parameter, $\beta = 0.727 \pm 0.014$; central electron density, $n_{e,0} = (1.46 \pm 0.26) \times 10^{-2} h_{70}^{-2} \text{cm}^{-3}$.

2 Global Parameters of Merging Clusters

Gas Mass Fraction

We show in Figure 2 the radial profile of the gas mass fraction, $f_{\text{gas}}(< r) = M_{\text{gas}}(< r) / M_{\text{tot}}(< r)$. We used the best-fitting models derived in §1 to calculate $f_{\text{gas}}(< r)$. Using the β model we extrapolated the gas mass profile

outside $\theta = 6'$ where the weak lensing mass profile is available. The values within typical radii of r_{2500} , r_{500} and r_{vir} , at which the mean density is 2500, 500 and δ_{vir} times the critical density of the universe, are $f_{2500} = 0.108$, $f_{500} = 0.133$ and $f_{\text{vir}} = 0.165$, respectively. The central gas mass fraction, f_{2500} , is similar to those values for relaxed clusters derived by X-ray data alone, such as 0.091 ± 0.002 (Vikhlinin et al. [7]) and 0.117 ± 0.002 (Allen et al. [1]). The values of f_{500} deduced from X-ray studies show a large scatter among different clutters and different observations. We note the values of f_{500} deduced from X-ray studies show a large scatter among different clutters and different observations. We found the virial gas fraction, f_{vir} , of A1914 is consistent with the cosmic mean baryon fraction Ω_b/Ω_m , constrained by the CMB observations (Spergel et al. [5]). The virial gas fraction, f_{vir} , is consistent with the cosmic mean baryon fraction Ω_b/Ω_m , constrained by the CMB observations (Spergel et al. [5]). We emphasize that a combined weak-lensing and X-ray study will allow us to determine gas mass fractions even in merging clusters.

$L_X - T$ relation

We derived the X-ray bolometric luminosity $L_{X,\text{bol}}$ and temperature T with a single-temperature model. The resulting X-ray luminosity within r_{200} is $L_{X,\text{bol}} = 2.5 \times 10^{45} h_{70}^{-2} \text{ergs s}^{-1}$ with $k_B T_{\text{vir}} = 4.7_{-0.3}^{+0.3} (M/M_{\text{vir}})^{2/3} \text{keV}$, which is consistent with the observed local $L_X - T$ relation from previous X-ray studies: $L_{X,\text{bol}}(< r_{200}) = 2.3_{-0.3}^{+0.3} \times 10^{45} (k_B T/9.6 \text{keV})^{2.88 \pm 0.15} h_{70}^{-2} \text{ergs s}^{-1}$ (Arnaud & Evrard [2]). This indicates that the observed local $L_X - T$ relation holds even in the merging cluster A1914.

$M - T$ relation

The observed temperature $k_B T = 9.6 \pm 0.3 \text{keV}$ is significantly higher than the virial temperature, $k_B T_{\text{vir}} = 4.7_{-0.3}^{+0.3} (M/M_{\text{vir}})^{2/3} \text{keV}$ derived from the weak lensing analysis. If the cluster were virialized before the merging process, then the ICM temperature could be heated up by a factor of two. Based on this scenario, we constrain the heating energy of the ICM induced by the cluster merger as

$$\langle \Delta E_{\text{ICM}}(r < 5') \rangle = 4\pi(k_B T_{\text{ave}} - k_B T_{\text{vir}}) \int \sum_j n_j(r) r^2 dr \sim 2 \times 10^{62} \text{erg},$$

with $n_H = 0.82n_e$, where we assumed the electron and ion temperatures are the same.

References

1. Allen, S. W. et al. 2004, MNRAS, 353, 457.
2. Arnaud, M. & Evrard, A. E. 1999, MNRAS, 305, 631.
3. Navarro, J. F., Frenk, C. S. & White, S. D. M. 1997, ApJ, 490, 493.
4. Okabe, N. & Umetsu, K. PASJ submitted.
5. Spergel, D. N. et al. 2003, ApJS, 148, 175.
6. Umetsu, K. & Okabe, N. : in prep.
7. Vikhlinin, A. et al. 2006, ApJ, 640, 691.